Full-field stress analysis by holographic phase-stepping implementation of the photoelastic-coating method — Source link ↗

T. Lyubenova, Elena Stoykova, Branimir Ivanov, W. Van Paepegem ...+2 more authors

Institutions: Bulgarian Academy of Sciences, Ghent University

Related papers:

- Recent advances in temporal phase-shifting speckle interferometry

- Phase-shifting speckle interferometry: a noise reduction filter for phase unwrapping

- Least-squares phase estimation with multiple parameters in phase-shifting electronic speckle pattern interferometry.

- Full field residual stress determination using hole-drilling and electronic speckle pattern interferometry (ESPI) with phase unwrapping method

- Phase measurement in temporal speckle pattern interferometry: comparison between the phase-shifting and the Fourier transform methods.

Full-field stress analysis by holographic phase-stepping implementation of the photoelastic-coating method

T Lyubenova[1], E Stoykova[1], B Ivanov[1], W Van Paepegem[2], A Degrieck[2] and V Sainov[1]

[1]Institute of Optical Materials and Technologies, Bulgarian Academy of Sciences
Acad.G.Bonchev Str., Bl.101,1113 Sofia, Bulgaria
[2]Ghent University, Dept. of Mechanical Construction and Production,
Sint-Pietersnieuwstraat 41, 9000 Gent, Belgium

E-mail: t_lubenova@yahoo.com

Abstract. The paper describes a system for polariscopic and holographic phase-shifting implementation of the photolastic-coating method for full-field stress analysis. The easiest way to build the combined system is to use a laser light source. However, coherent illumination introduces a signal dependent speckle noise which worsens the accurate phase estimation and unwrapping. To answer the question how it affects the phase retrieval of isochromatics, isoclinics and isopachics, we modeled in the presented report the phase-shifting photoelastic measurement in the presence of speckle noise through calculation of the complex amplitudes in a Mach-Zender interferometer combined with a circular polariscope and made denoising of simulated and experimental fringe patterns. The latter were recorded at pure tensile load for PhotoStress coated samples with a mechanical stress concentrator.
42.40.Kw, 42.30.Rx, 42.30.Ms

1. Introduction.

A holographic phase-shifting realization of the photolastic-coating method [1-3] is an effective approach to separate the stress components over the tested specimen due to its easier and faster implementation in comparison with the oblique-incidence method, the strip coating method and the strain gage separation method [4-5]. For the purpose, a series of six photoelastic fringe patterns (FPs) are recorded at preliminary known orientations of the polarization elements in a circular polariscope to build both isochromatic and isoclinic phase maps which give the loci of points with a constant difference of the principal stresses and a constant principal stress direction respectively. In addition, holographic recording of four FPs is performed for retrieval of isopachic fringes which give the sum of the principal stresses. If a two-load phase-shifting technique is applied for unambiguous phase retrieval, the number of the required FPs doubles [6]. This strengthens the requirements set on the accuracy of the phase retrieval and on the signal-to-noise ratio in the recorded FPs.

The easiest way to perform combined polariscopic and holographic measurement for full-field stress analysis is to use a laser light source. However, coherent illumination introduces a signal dependent speckle noise which worsens the accurate phase estimation and unwrapping. To answer the question how it affects the phase retrieval of isochromatics, isoclinics and isopachics, we modeled in the presented report the phase-shifting photoelastic measurement in the presence of speckle noise through calculation of the complex amplitudes in a Mach-Zender interferometer combined with a circular polariscope and made denoising of simulated and experimental FPs. The latter were recorded at pure tensile load for PhotoStress coated samples with a mechanical stress concentrator.

2. Experimental set-up and light intensity equations

The schematic diagram of the system we have built for two-dimensional holographic photoelastic measurement of isochromatics/isopachics in reflection mode is depicted in figure 1. The light source was a DPSS CW generating laser which emitted a vertically polarized light at 532 nm. We use P, Q, and A to denote a polarizer, a quarter-wave (retardation) plate, and an analyzer, respectively; the subscript indicates the angle formed by the transmission axis of the polarizers or by the fast axes of the retardation plates with the reference axis X. The first quarter-wave plate $Q_{\pi/4}$ was positioned at the output of the laser to produce a circularly polarized light which was collimated by the lens L_2 after the beam expander (lens L_1) and the spatial pinhole filter (SF). A 10% beam splitter formed the two arms of a Mach-Zender interferometer with the 90 percents of light used to illuminate the object and the remaining 10% redirected as a reference beam. The sample was illuminated normally to its surface and observed using one and the same 50% beam splitter. When the shutter in the reference beam was closed, the system operated as a circular polariscope for photoelastic measurement of isochromatics and isoclinics. The phase steps were introduced by rotation of the second quarter-wave plate Q_γ and the analyzer A_β. Accuracy of rotation was $\pm$ 0.1 degree. For the isopachic measurement the shutter was open and the interference patterns of the object and reference beams were recorded after the second 50% beam splitter, at different phase shifts, produced by rotation of Q_γ and parallel transmission axes of the analyzer A_β and the polarizer P_α. The objective L_3 formed image plane recording of the fringe patterns. The whole system was assembled on a vibration insulated holographic table. The loading device was also positioned on the holographic table. The fringe patterns were recorded with a Baumer Optics CCD camera with 782x582 pixels.
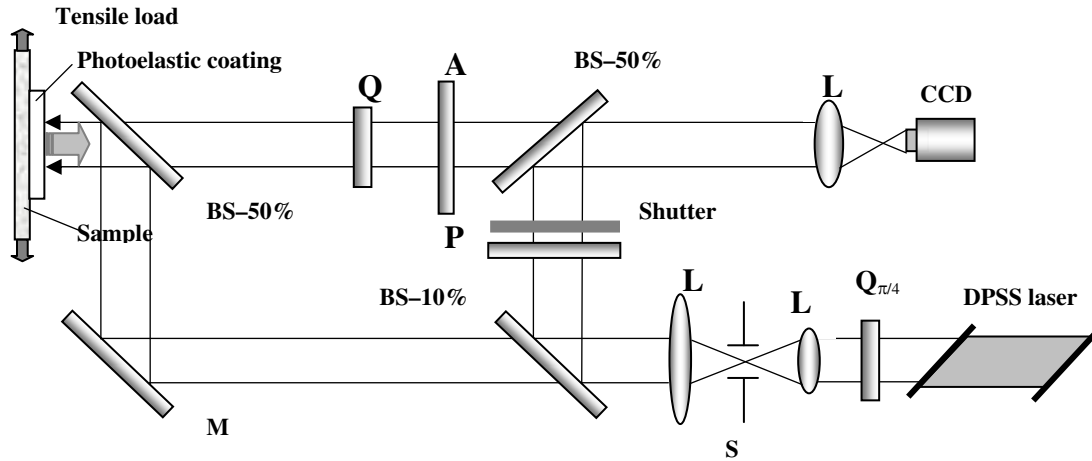

Figure 1 Optical set-up for phase-shifting holographic photoelastic measurement of isochromatics, isoclinics and isopachics. L_1 – beam expander, L_2 – collimator, L_3 – objective, SF – spatial filter, BS – beam-splitter, M – mirror, Q – quarter-wave plate, P – polarizer, A – analyzer.

A birefringent sample $R_{\delta,\theta}$ whose principal stress σ_1 direction subtends an isoclinic angle θ with the reference axis X is characterized with the following Jones matrix:

$$R_{\delta,\theta} = \begin{bmatrix} e^{i\delta_1}\cos^2\theta + e^{i\delta_2}\sin^2\theta & \left(e^{i\delta_1} - e^{i\delta_2}\right)\sin\theta\cos\theta \\ \left(e^{i\delta_1} - e^{i\delta_2}\right)\sin\theta\cos\theta & e^{i\delta_2}\cos^2\theta + e^{i\delta_1}\sin^2\theta \end{bmatrix} \tag{1}$$

where $\delta_{1,2}$ are the phase retardations along the directions of the principal stresses, $\sigma_{1,2}$, of the specimen, respectively. Determination of the difference and the sum of both phase retardations allows for evaluation of the difference and the sum of the principal stresses, $\delta_d = \delta_1 - \delta_2 = Ctk(\sigma_1 - \sigma_2)$ and $\delta_s = \delta_1 + \delta_2 = Dtk(\sigma_1 + \sigma_2)$, where $k = 2\pi/\lambda$ and λ is the laser wavelength, t is the thickness of the sample, and C and D are the optical constants of the sample. The parallel, E_p, and normal, E_n, to the analyzer axis components of the light vector can be described as

$$\begin{pmatrix} E_p \\ E_n \end{pmatrix} = A_\beta Q_\gamma R_{\delta,\theta} Q_{\pi/4} P_\alpha E_0 \tag{2}$$

where E_0 is the amplitude of the light vector, and α, β and γ are the angles, subtended by the transmission axes of the polarizer, the analyzer and the fast axis of the quarter-wave plate with the reference axis X. The angle α takes only values 0 and π/2. The Jones matrices in (2) are given by

$$A_\beta = \begin{bmatrix} \cos\beta & \sin\beta \\ -\sin\beta & \cos\beta \end{bmatrix}, \quad Q_\gamma = \frac{\sqrt{2}}{2} \begin{bmatrix} 1 + i\cos 2\gamma & i\sin\gamma \\ i\sin\gamma & 1 - i\cos 2\gamma \end{bmatrix} \tag{3}$$

The intensity recorded at a given pixel of the CCD camera is $I = E_p E_p^*$ where asterisk denotes a complex conjugate. For a closed interferometric channel we have $P_{\pi/2}$ in (2). The values of β and γ as well as the light intensity equations are given in [3,7]. From these equations one readily obtains the formulas for calculation of the wrapped phase maps of isoclinics, isochromatics and isopachics:

$$\theta = \frac{1}{2} arctg \left(\frac{I_3 - I_5}{I_6 - I_4} \right), \quad \sin\delta_d \neq 0 \tag{4}$$

$$\tan\delta_d = \frac{(I_3 - I_5)\sin 2\theta + (I_6 - I_4)\cos 2\theta}{I_2 - I_1} \tag{5}$$

$$\delta_s = \frac{1}{2} \arctan\left\{ \frac{I_7 - I_8 + I_9 - I_{10}}{I_7 + I_8 - I_9 - I_{10}} \right\} \quad \text{at} \quad \cos(\delta_d/2)\cos 2\theta \neq 0 \tag{6}$$

where the intensities $I_1 \div I_{10}$ correspond to different combinations of α, β and γ. For correct unwrapping of the phase maps (4)-(6) we applied the two-loading method [6].

To describe analytically the impact of the speckle noise on the recorded FPs, we assumed that the complex amplitude after reflection of the laser beam from the photoelastic sample is a random phasor sum [8] and modeled the speckle noise as a delta-correlated circular Gaussian process in the location of the specimen with the Jones vector of light just after reflection from the specimen given by

$$E_{\delta,\theta} == \frac{\sqrt{2}}{2} e^{i\delta_2} u_0 \begin{bmatrix} (a_{11}a_{sp} - a_{12}b_{sp}) + i(a_{12}a_{sp} + a_{11}b_{sp}) \\ (a_{21}a_{sp} - a_{22}b_{sp}) + i(a_{22}a_{sp} + a_{21}b_{sp}) \end{bmatrix} \tag{7}$$

where u_0 was the amplitude of the laser light field, a_{sp}, b_{sp} were calculated as $N(0, 0.5)$ random numbers, with $N(a, s^2)$ being an independent Gaussian variable with a mean a and variance s^2, and the coefficients $a_{11}, a_{12}, a_{21}, a_{22}$ for the case of isochromatics are given by

$$\begin{aligned} a_{11} &= \cos\theta(\sin\Theta^- - \sin\theta) & a_{12} &= \cos\theta\cos\Theta^- + \sin^2\theta \\ a_{21} &= \sin\theta(\cos\Theta^- - \cos\theta) & a_{22} &= \sin\theta\sin\Theta^- + \cos^2\theta \end{aligned} \tag{8},$$

whereas for the case of isopachics by

$$\begin{aligned} a_{11} &= \cos\theta\cos\Theta^+ + \sin^2\theta & a_{12} &= \cos\theta(\sin\Theta^+ - \sin\theta) \\ a_{21} &= \sin\theta\sin\Theta^+ + \cos^2\theta & a_{22} &= \sin\theta(\cos\Theta^+ - \cos\theta) \end{aligned} \tag{9}$$

where $\Theta^\mp = \theta \mp \delta_d$. The real and imaginery parts of the complex amplitudes at the output of the set-up in figure 1 for isochromatics and isopachics are given in [3]. From the complex amplitudes one easily obtains the expressions for the intensities which are recorded by the CCD camera in the presence of speckle noise. In the case of the interferometric measurement (FPs $I_7 \div I_{10}$) one should take into account the reference beam with the complex amplitude $U_0 \exp(i\varphi_0)$.

3. Denoising of fringe patterns

We simulated the combined polariscopic-holographic measurement for an epoxy resin disk with a radius 21.2 mm, thickness 6 mm, $C = 52.1 \times 10^{12} \text{m}^2\text{N}^{-1}$ and $D = 217.3 \times 10^{12} \text{m}^2\text{N}^{-1}$ under concentrated diametral compression. The wavelength was 532 nm. The applied two loads were 350 N and 355 N. The simulated image size in the plane of the sample was 1024×1024 pixels. The free propagation after the sample to the second quarter-wave plate was modeled in Fresnel approximation [9] with a complex amplitude of the light falling on the quarter-wave plate given by $U_{QW}(x,y) = FFT^{-1}\{H \cdot FFT[U_s(x,y)]\}$, where $U_s(x,y)$ is the complex amplitude after the sample, H is the coherent transfer function of the free space and $FFT[..]$ denotes the Fourier transform. We modeled also the integration by the CCD camera within a window 2×2 pixels, so the size of the recorded image was 512×512 pixels. The spacing of the interferometric pattern was 0.6 mm. In the simulation we kept the ratio 9:1 between the beam illuminating the object and the reference beam.

We applied the following denoising algorithms: 1) median filtering, 2) a James-Stein filter after homomorphic transformation of the signal [10], and 3) filtering with an annual filter in the frequency domain after normalization of the fringe pattern [11]. The first two filters yielded smooth profiles of the recorded intensity if the size of the averaging window was greater than 12x12 pixels. The second filter provided better results. The drawback of using large filtering windows is that the estimates of the intensities $I_1 \div I_{10}$ are negatively or positively biased. However, since the biases in different estimates are more or less correlated and the input data for (4)-(5) are not the intensities but their differences, one can achieve satisfactory accuracy of phase retrieval of isochromatics and isoclinics. To illustrate this statement, we present in figure 2 one-dimensional profiles of the differences $I_2 - I_1$, $I_3 - I_5$ and $I_6 - I_4$ for the noiseless fringe patterns and the speckled patterns after averaging with a James-Stein filter in a window of 15x15 pixels. The profiles are taken along a line 9 mm below the top of the disk to be comparatively far away from the point of force application. Since the simulation has been made for a concentrated force applied to a point, $\sigma_1 \pm \sigma_2$ experiences rapid increase in its vicinity, making determination of $\delta_{s,d}$ close to it unreliable. Figure 2 exhibits good coincidence between the filtered profiles and the noiseless ones. Figures 3 a and 3 c show the profiles of δ_d and θ taken along the same line as in figure 2 from the noiseless and filtered unwrapped isochromatic and isoclinic phase maps. Figures 3 b and 3 d present the histograms of the differences between the noiseless and filtered values. As it can be seen, the error for estimation of isochromatics is spread between -0.04 rad and 0.01 rad whereas for the isoclinics it is within the interval (-0.05, 0.05) radians. The expression for δ_s contains the intensities $I_7 \div I_{10}$ both in the nominator and denominator, and some of them are included with opposite signs. We obtained much better result if denoising was applied directly to $I_7 - I_8 + I_9 - I_{10}$ and $I_7 + I_8 - I_9 - I_{10}$ than to each of the FPs separately. Nevertheless, the error in determination of isopachics occupies greater interval (figures 3 e and 3 f) in comparison with determination of δ_d and θ.
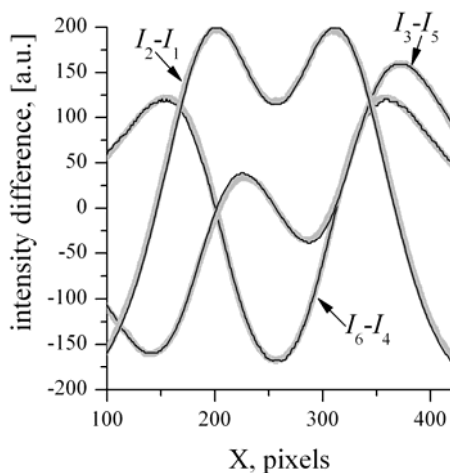

Figure 2 One-dimensional distributions of intensity differences along the X axis at 9 mm below the top of the disk under unidirectional compression; X axis is normal to the direction of the applied force (grey line – noiseless profile, black line – filtered profile).
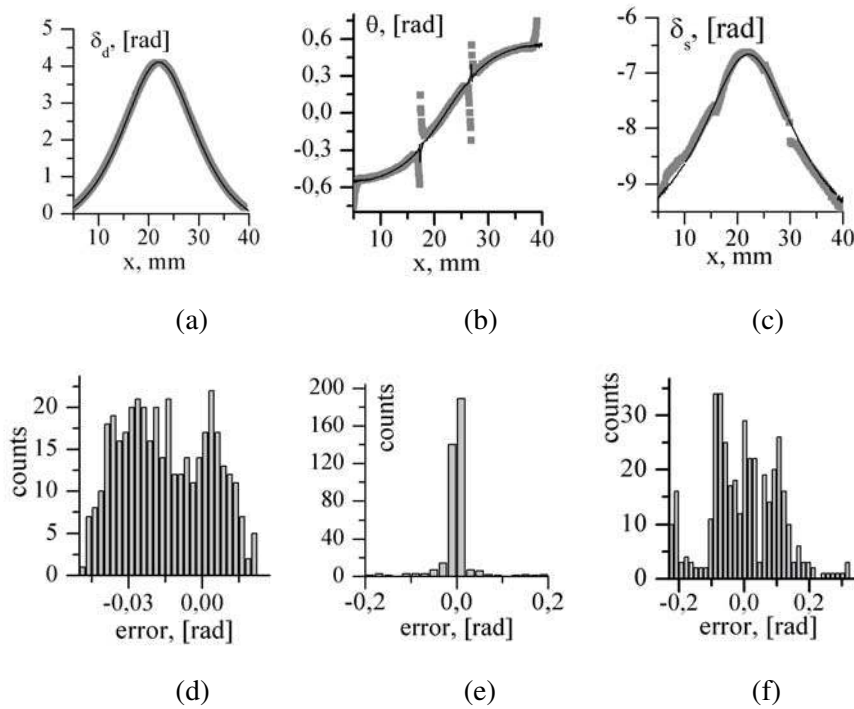
(a)   (b)   (c)

(d)   (e)   (f)

Figure 3 One-dimensional unwrapped distributions of δ_d, θ and δ_s (a,c,e) along the X axis at 9 mm below the top of the disk under unidirectional compression (grey line – calculation from noiseless FPs, black line – calculation from the filtered FPs); histograms of errors in determination of δ_d, θ and δ_s (b,d,f) from the filtered FPs.

4. Filtering of experimental fringe patterns.

The performed photoelastic experiment included measurement of isochromatics/isopachics of a window security film with different stress concentrators at pure tensile loading. The studied samples were with a length 235 mm and width 20 mm. The thickness of the tested film was 0.1 mm. We used a thick PhotoStress® coating [12] to induce birefringence. Installation of the coating on the sample was made using adhesives of the producer. We measured the patterns for a film with a hole with a diameter of 6 mm in the middle as a stress concentrator.
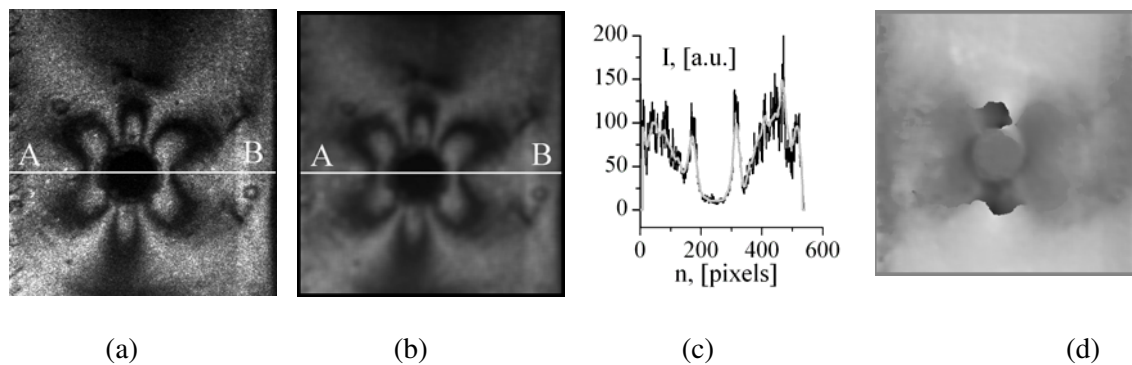

(a)   (b)   (c)   (d)

Figure 4 (a,b) 8-bit images of the noisy and filtered FP I_2; (c) intensity profiles along the line AB for the noisy (black line) and the filtered (grey line) FPs; (d) 8 bit image of the unwrapped isochromatics phase map.

Figure 4 shows the effect of denoising of an experimental FP corresponding to I_2 recorded at loading 20 N with the James-Stein filter with the size of averaging window 12x12. Figure 4 c gives the intensity

profile along the line AB. Successful retrieval of the isochromatic phase map is presented in figure 4 d. The obtained distribution of $\sigma_1 - \sigma_2$ is smooth and consistent with the theory. Figure 5 a depicts the FP I_7 recorded for the same sample and same loading for calculation of isopachics after filtering with the James-Stein filter within a window of 15×15 pixels. Filtering was performed after normalization of the fringe patterns in the frequency domain [11]. The filter failed to remove the line noise observed in the recorded images $I_7 \div I_{10}$ (see figure 5b). To remove this noise we applied another approach – normalization and filtering with an annual filter in the frequency domain with inner and outer radii 4 and 70 pixels. The result of this procedure is shown in figures 5 c and d which exhibit substantial improvement in the quality of the filtered image.
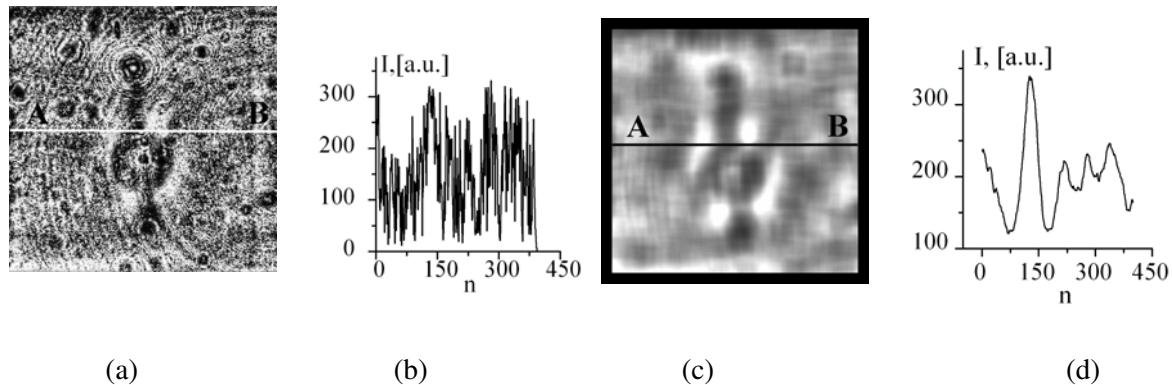

| (a) | (b) | (c) | (d) |

Figure 5 (a) 8 bit image of the normalized and filtered with the James-Stein filter FP I_7; (b) intensity profile along line AB in figure (a); (c) 8 bit image of the normalized and filtered with the annual filter in the frequency domain FP I_7; (d) intensity profile along line AB in figure (c).

In summary, we proved by simulation the possibility for accurate measurement of isochromatics/isopachics using combined holographic polariscopic system with coherent light source. Accuracy of phase retrieval of isochromatics and isoclinics from properly filtered and normalized FPs is completely acceptable. Processing of the experimental data confirmed this conclusion. Retrieval of isopachics is more vulnerable to speckle noise and requires additional refinement of the filtering procedure.

References

[1]   Yoneyama S, Morimoto Y, and Kawamura M 2005 *Meas. Sci. Technol.* **16** 1329–1334
[2]   Stoykova E, Lyubenova T, and Sainov V 2011 *Proc. SPIE* **7747** 77470N-1-10
[3]   Dulieu-Barton J, and Quinn S 2008 *Appl. Mech. Mat.* **3 – 4** 229-234
[4]   Solaguren-Beascoa Fernández M, Alegre Calderon J, Bravo Diez P, and Cuesta Segura I 2010 *J. Strain Anal. Eng. Des.* **45**, 1-17
[5]   Tong L, Asundi A, and Boay C 2000 *Opt. Eng.* **40** 1629-1635
[6]   Lei Z, Yun H, Yun D, and Kang Y 2007 *Opt. Las. Eng.* **45** 77–82
[7]   Goodman J 2008 *Speckle Phenomena in Optics: Theory and Applications* (USA: Roberts&Company Publishers)
 [9]   Equis E, and Jacquot P 2006 *Proc. SPIE* **6341** 634138-1-6
[10]   Terrillon J-C 1996 *Appl.Opt.* **31** 1879-1893
[11]   Ochoa N, and Silva-Moreno A 2007 Opt. Commun. 270, 161–168 ()
[12]   Tech Note TN-70202, http://www.vishaymg.com/